

Effect of Ni proportion on the performance of proton exchange membrane fuel cells using PtNi/C electrocatalysts

Fernanda T. da Silva · Vicenti A. Dalmazzo · Márcia R. Becker ·
Michèle O. de Souza · Roberto F. de Souza · Emilse M. A. Martini

Received: 24 May 2013 / Revised: 27 July 2013 / Accepted: 3 August 2013 / Published online: 28 August 2013
© Springer-Verlag Berlin Heidelberg 2013

Abstract PtNi/C electrocatalysts were synthesised by borohydride method on functionalised carbon support. Energy-dispersive X-ray spectroscopy, X-ray diffraction, transmission electron microscopy and both cyclic and linear voltammetry were employed to characterise the composition, crystalline structure, morphology and catalytic properties of the PtNi/C electrocatalysts. Different Ni proportions in the PtNi/C electrocatalysts were evaluated in the cathode or anode in a H₂/air proton exchange membrane fuel cells (PEMFC) by polarisation curves. PtNi particles uniformly dispersed with different proportions of metals obtained. The increase of Ni proportion in the electrocatalyst led to materials with higher mass activity values toward the oxygen reduction reaction and a greater electrochemical-active surface area. PtNi/C electrocatalysts in the cathode presented higher mass activity values at high potential in the PEMFC. The best PEMFC performance was obtained with PtNi 13 at.% Ni (cathode) and Pt/C (anode) relative to the Pt/C (cathode and anode) with identical Pt loadings. PtNi/C electrocatalysts in PEMFC may be used as an alternative to Pt/C electrocatalyst.

Keywords Alloy catalysts · Fuel cell · Electrocatalyst · Borohydride method · PtNi/C · PEMFC

Introduction

Fuel cells are promising alternative energy sources because of their negligible pollution generation and flexibility within

various applications. When fed with pure hydrogen fuel while using air as an oxidant, the only reaction products are water, heat and power. This type of system may be part of a sustainable cycle that uses hydrogen as a clean energy vector, which is the basis of the hydrogen economy.

Fuel cells are devices that convert chemical energy into electrical energy through highly efficient reduction and oxidation reactions. Proton exchange membrane fuel cells (PEMFCs) are devices that operate at low temperatures (until 80 °C). Currently, the most popular membrane used for proton conduction is Nafion[®], which is a perfluorinated polyolefin chain with pendant sulphonic acid groups.

Many types of electrocatalysts have been described for application in PEMFCs, but those involving platinum nanoparticles on carbon support are the most prominent due to their intrinsic activity and stability [1, 2]. Pt-PEMFCs show high catalytic activity for both hydrogen oxidation reactions and oxygen reduction reactions (ORRs) but have drawbacks including high cost, limited availability of the noble metal and deactivation of the catalyst by CO that may be contaminating the hydrogen. Many researchers have focused on improving PEMFC performance, including the use of alternative materials as electrocatalysts [3–5].

Binary or ternary alloys containing Pt are an attractive alternative for PEMFC electrodes. This approach allows utilise less platinum while maintaining the high performance of the fuel cell [6–8]. Several alloys containing transition metals and Pt have exhibited significantly higher catalytic activities than pure platinum. These materials have been synthesised with Co, Ru, Cr, Pd, W, Sn, Au and Ni [3, 7, 9–29]. These alloys may be obtained by various methods, obtaining different electrocatalysts in their morphologies, dispersions, compositions and performances [4, 12–20]. The borohydride reduction method has been successfully used to prepare PtNi/C alloys with a nickel content of up to 50 at.% [11]. The electrocatalytic activity of these materials may exceed the activity of the Pt/C electrocatalyst when utilised in direct

F. T. da Silva · V. A. Dalmazzo · M. R. Becker · M. O. de Souza ·
R. F. de Souza · E. M. A. Martini (✉)
Instituto de Química, Laboratório de Reatividade e Catálise,
Universidade Federal do Rio Grande do Sul, Prédio 43131, Sala 119,
Av. Bento Gonçalves 9500, 91501-970 Porto Alegre, RS,
P.O. Box 15003, Brazil
e-mail: emilse@iq.ufrgs.br

methanol oxidation [10]. PtNi/C electrocatalysts have also proven to be more stable and active than Pt/C electrocatalyst in the ORR [13, 19]. Several authors reported the catalytic activity of electrocatalysts only in half-cell in acidic or basic media. Full technological assessment of these materials requires that they be evaluated in a fuel cell. To the best of our knowledge, there are no reports comparing the performance of a PEMFC with electrodes utilising different proportions of Ni in PtNi/C electrocatalysts obtained by borohydride reduction method. The aim of this work is to present the effect of Ni proportion on the performance of the PEMFC using H₂/air and PtNi/C electrocatalysts synthesised by borohydride method as anode and/or cathode.

Experimental

PtNi/C electrocatalysts were prepared by borohydride method [19, 21–25] with 20 wt.% metal loading on Vulcan XC-72R carbon (Cabot, 240 m² g⁻¹). The precursors, hexachloroplatinic acid (IV) hexahydrate (H₂PtCl₆·6H₂O, Merck) and nickel (II) chloride hexahydrate (NiCl₂·6H₂O, 98 %, Synth) were dissolved in a mixture of water/isopropanol 1:1 (v/v) and the Vulcan carbon previously treated with HNO₃ was added [22]. The metals were reduced using sodium borohydride (NaBH₄, 95 %, Vetec) at 25 °C for 30 min. The mixture was filtered and the solid was washed with water and dried at 70 °C for 2 h.

The relative proportions of the Vulcan carbon, platinum and nickel, as well as the material's homogeneity were obtained by energy-dispersive X-ray spectroscopy (EDX) coupled with scanning electronic microscope on a JEOL-JSM 5800 with a 20 kV incident electron beam. The precision for these weight ratios was ±3 %.

The crystalline structure, parameter lattice and Ni atomic fraction of the PtNi/C electrocatalysts were obtained by X-ray

Table 1 Characterisation of Pt/C and synthesised PtNi/C electrocatalysts by EDX and DRX analyses

Electrocatalyst	Metal loading wt.% (±3)	Ni at.% (±3)	2θ (220) degree (±0.1)	a _{fcc} Å (±0.003)	x _{Ni} at.%
Pt/C	20	0	67.5	3.919	0
PtNi/C 15	18	13	68.2	3.886	8
PtNi/C 25	15	24	68.7	3.861	15
PtNi/C 45	17	44	69.2	3.836	21

diffraction. The X-ray diffractograms were obtained using a D500 Rigaku diffractometer (Siemens) operating at a scan rate of 0.05° s⁻¹ in the range of 2θ = 20–90° using CuK_α radiation (1.54056 Å).

The dispersion of the metals on the carbon support and the particle size distribution obtained by counting at least 600 nanoparticles was analysed by transmission electron microscopy (TEM) using a JEOL JEM 1200ExII microscope operating at 120 kV. The SigmaScan Pro 5 software was used to analyse the dispersion.

The electrochemical measurements were performed with an Autolab PGSTAT 30 potentiostat coupled with a GPES module in a half-cell in a conventional three-electrode electrochemical cell. A double junction saturated calomel electrode was used as the reference electrode, a Pt grid was used as the counter electrode and the synthesised electrocatalysts were used as the working electrodes. The potentials are presented relative to reversible hydrogen electrode (RHE). The working electrodes were prepared using the thin porous coating technique [24, 30] with ca. 10 mg electrocatalyst, 15 mg 5 wt.% Nafion[®] solution and 30 mg isopropanol and fixed onto a glassy carbon rotating disc electrode (GCRDE). The cyclic

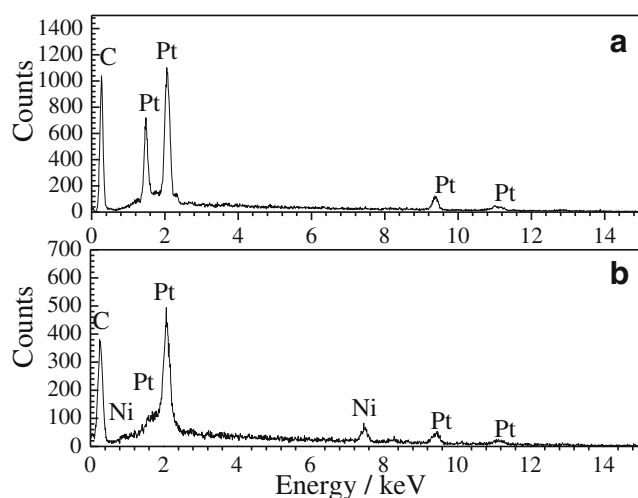


Fig. 1 EDX of Pt/C (a) and PtNi/C 45 (b) electrocatalysts

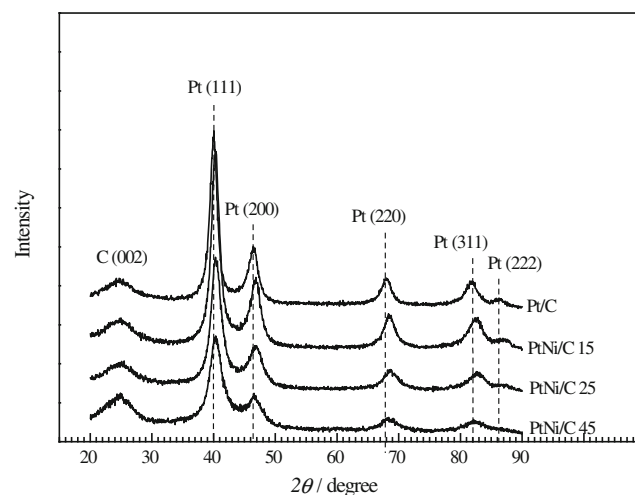


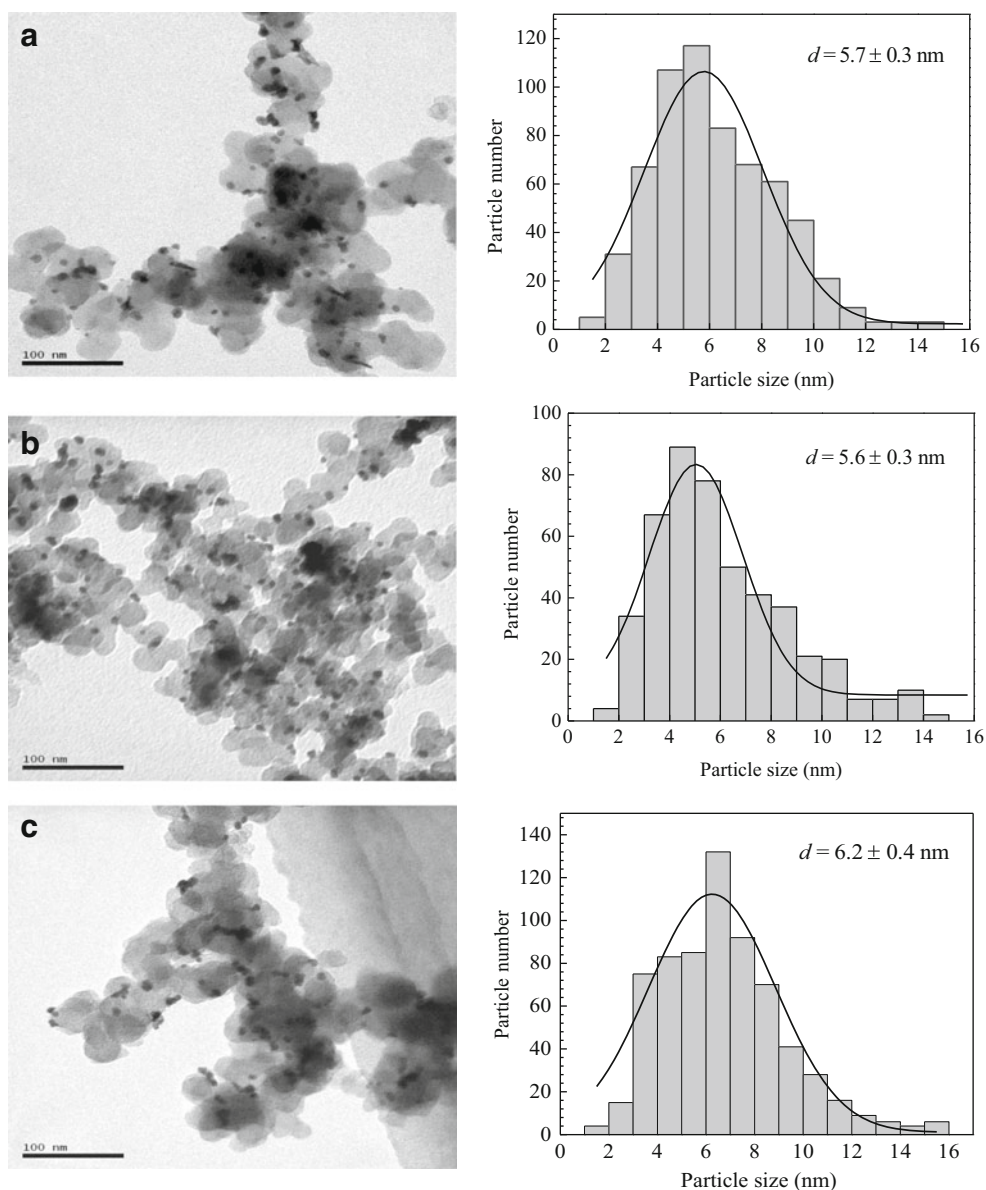
Fig. 2 X-ray diffraction patterns of Pt/C and synthesised PtNi/C electrocatalysts

voltammetry (CV) was recorded between -0.05 and $+0.95$ V RHE at a scan rate of 0.01 V s^{-1} in a de-aerated 0.5 mol L^{-1} H_2SO_4 solution. This cyclic voltammograms were recorded after 30 activation cycles with the GCRDE rotating at 1,000 rpm [24]. The electrochemical active surface area (S_{EAS}) was calculated using the charge of hydrogen desorption from the electrode surface, assuming that the charge for Pt is 0.21 mC cm^{-2} [20, 31]. The electrocatalyst's durability curves were determined using CV at 1,000 cycles, a scan rate of 0.02 V s^{-1} and 1,800 rpm [9]. The measurement of the mass activity for the ORRs (MA_{ORR}) was conducted in an air-saturated 0.5 mol L^{-1} H_2SO_4 solution at room temperature by linear voltammetry from $+0.92$ to $+0.61$ V RHE at 1,800 rpm. The mass activity was determined using the

current values obtained at 0.85 V and normalised using the weight of the Pt [24, 30] with a precision of ± 3 %.

The PEMFC performance was evaluated using a FC5-1H cell with a 4.84 cm^2 active area and a CDR50A-2 dynamic charge from Electrocell. PtNi/C electrocatalysts were used as the cathode or anode while the Pt/C electrocatalyst (20 wt.% Pt EC-20-PTC, Carbon XC-72) was held as a pattern in the opposite electrode. The electrodes were made by brushing technique with 0.5 mg Pt cm^{-2} and 30 wt.% of Nafion[®]. Nafion[®] 117 was used as the polymer membrane and was previously treated with H_2O_2 and H_2SO_4 . The membrane-electrode assemblies (MEAs) were prepared by hot pressing the electrodes onto the membrane at 125 °C and 50 kgf cm^{-2} for 2 min. The measurements were performed using

Fig. 3 TEM micrographs and particle size distributions of the PtNi/C 15 (a), PtNi/C 25 (b) and PtNi/C 45 (c)



independent H_2 (1 bar) and air (2 bar) feeds saturated with water at 85°C and flowing at 100 and 500 mL min^{-1} , respectively. The PEMFC performance was evaluated at 80°C . Each measurement was performed at least five times and the studied parameters were obtained with a precision of $\pm 2\%$. The polarisation curves were not corrected for the loss of internal resistance. The current values were expressed in Ampere per gram of platinum (mass activity) because the Pt loading was 0.5 mgPt cm^{-2} for all prepared MEAs.

Results and discussion

PtNi/C electrocatalysts were synthesised by direct reduction with sodium borohydride on functionalised carbon support. The EDX results show that materials were produced with metal ratios of 13, 24 and 44 at.% Ni in the total metal loading; the materials were named PtNi/C 15, PtNi/C 25 and PtNi/C 45, respectively. The EDX spectra in Fig. 1a,b show that Pt is present in Pt/C and coexists with Ni in PtNi/C 45 [10]. The metal loading on the functionalised carbon support was maintained between 15 and 18 wt.% as shown in Table 1. The metal composition varies less than 3 % across the five areas of each sample.

The crystalline structure, lattice parameter (a_{fcc}) and Ni atomic fraction in each PtNi alloy (x_{Ni}) were obtained by X-ray diffraction and the diffractograms are shown in Fig. 2. The diffractograms of the PtNi/C electrocatalysts show the same characteristic peaks as Pt/C. The carbon (002) support peak appears at $2\theta = 25^\circ$ and the Pt peak corresponding to the (111), (200), (220), (311) and (222) planes appear at $2\theta = 39.9^\circ$, 46.6° , 67.5° , 81.8° and 86.1° , respectively [14, 19, 32, 33]. These materials show face-centred cubic (fcc) structures characteristic of Pt metal. No peaks of metallic nickel or nickel oxides/hydroxides were observed [25] indicating the absence of segregated crystalline Ni phases. The peaks in the diffractograms for the PtNi/C electrocatalysts are slightly shifted to higher 2θ values relative to the corresponding peaks in the Pt/C electrocatalyst. The (220) peak shifts from 67.5° (Pt/C) to 69.2° (PtNi/C 45). Therefore, all of the PtNi/C electrocatalyst samples have the same crystalline structure and the slight shifts indicate that alloys incorporating Ni into the Pt crystalline structure were formed. The formation of the PtNi alloys is in reasonable agreement with the recently reported results [34].

The a_{fcc} were calculated using the (220) peak as a reference. The obtained values (Table 1) show a decrease that was proportional to the increase in the Ni content of the electrocatalysts: being from 3.919 \AA (Pt/C) to 3.836 \AA (PtNi/C 45). This indicates that there was a contraction of the crystalline lattice. These results corroborate the inclusion of Ni in the crystalline structure of Pt because Ni has a smaller atomic radius.

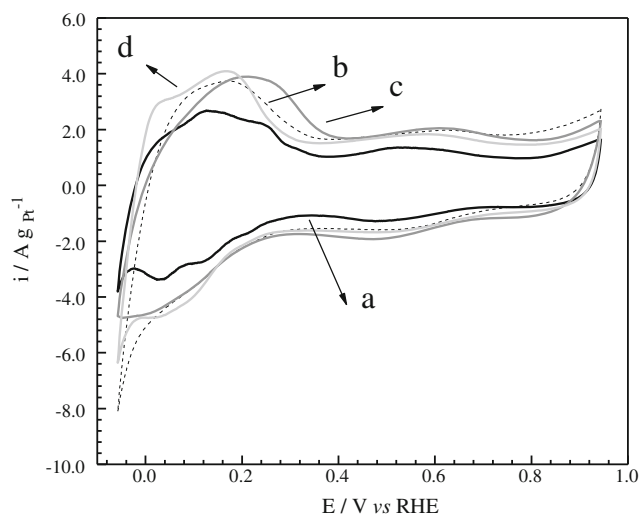


Fig. 4 Cyclic voltammograms for the Pt/C (a), PtNi/C 15 (b), PtNi/C 25 (c) and PtNi/C 45 (d) in de-aerated $0.5\text{ mol L}^{-1}\text{ H}_2\text{SO}_4$ with a scan rate of 0.01 V s^{-1} at 1,000 rpm

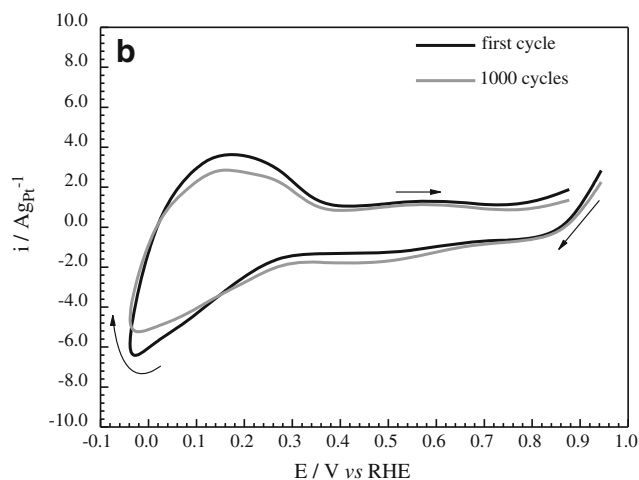
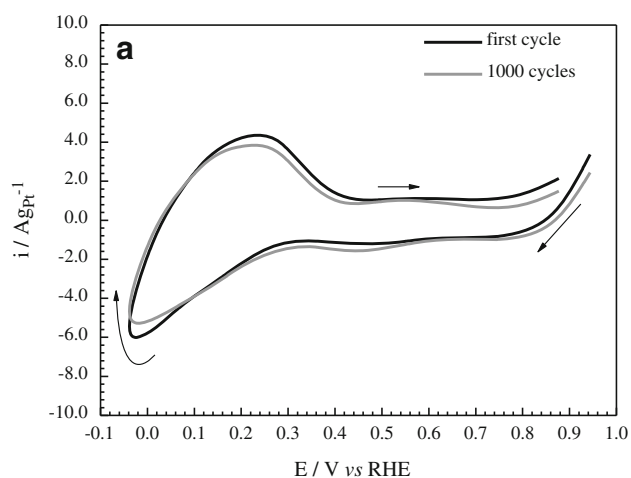


Fig. 5 Electrocatalyst's durability curves for the Pt/C (a) and PtNi/C 45 (b) in de-aerated $0.5\text{ mol L}^{-1}\text{ H}_2\text{SO}_4$ with a scan rate of 0.02 V s^{-1} at 1,800 rpm

Table 2 Arrangement of different PtNi/C electrocatalysts in the MEAs

MEA	Pt AC	PtNi 15-C	PtNi 25-C	PtNi 45-C	PtNi 15-A	PtNi 25-A	PtNi 45-A	PtNi 15-AC
Cathode	Pt/C	PtNi/C 15	PtNi/C 25	PtNi/C 45	Pt/C	Pt/C	Pt/C	PtNi/C 15
Anode	Pt/C	Pt/C	Pt/C	Pt/C	PtNi/C 15	PtNi/C 25	PtNi/C 45	PtNi/C 15

The Ni atomic fraction in the x_{Ni} is defined by Eq. 1 [19]:

$$x_{\text{Ni}}(\text{at.}\%) = \left(\frac{(a_0 - a)}{(a_0 - a_s)} \right) x_s \cdot 100 \quad (1)$$

where a_0 is the lattice parameter for Pt (3.919 Å), a_s is the lattice parameter for Pt₃Ni (3.820 Å) with 25 % of x_{Ni} and x_s is the Ni atomic fraction (0.25) [19]. The x_{Ni} content was calculated for every electrocatalyst (Table 1). The x_{Ni} varied between 8 at.% (PtNi/C 15) and 21 at.% (PtNi/C 45). The amount of incorporated Ni in the crystalline lattice is lower than the total Ni content observed by EDX. This difference in the Ni proportion in the samples is attributed to the formation of amorphous metallic or oxidised Ni outside of the Pt crystalline structure. These electrocatalysts present a higher x_{Ni} value than similar, previously described materials [14, 19].

The TEM analyses, as shown in Fig. 3, revealed spherical nanoparticles uniformly dispersed across the carbon, including metal particles (in black) and the carbon support (in grey). The average particle size (d) was 5.6 (PtNi/C 15) or 6.2 nm (PtNi/C 45). Therefore, the average particle size and distribution of the metal on the carbon support were not significantly affected by Ni proportion in the PtNi/C electrocatalysts.

Electrochemical measurements in a half-cell were used to determine the catalytic activity of the PtNi/C electrocatalysts in the acidic medium. The CVs of the Pt/C and PtNi/C electrocatalysts are shown in Fig. 4.

As expected, the hydrogen adsorption/desorption on the Pt was observed from -0.05 to $+0.4$ V vs. RHE. The hydrogen adsorption/desorption peaks for the PtNi/C electrocatalysts were not well defined. These findings validate the presence of polycrystalline electrocatalysts with disordered surface structures [15]. The S_{EAS} obtained were $29 \text{ m}^2 \text{ g}^{-1}$ Pt, $43 \text{ m}^2 \text{ g}^{-1}$ Pt, $51 \text{ m}^2 \text{ g}^{-1}$ Pt and $55 \text{ m}^2 \text{ g}^{-1}$ Pt to Pt/C, PtNi/C 15, PtNi/C 25 and PtNi/C 45, respectively. These values agreed with those found in previous reports [35]. The results show that the S_{EAS} increased when the Ni proportion relative to Pt was increased from 13 to 44 at.%. As expected, the Ni increased catalytic activity of the platinum in the hydrogen adsorption/desorption because the Pt–Pt bond (geometric effect) distance decreases and the 5d-band vacancy of Pt increases for Pt alloys (electronic effect) [36].

The electrocatalyst's durability curves indicated that there was no change in the shape of the voltammetric curve as observed in Fig. 5a,b for Pt/C and PtNi/C 45. The hydrogen adsorption/desorption peaks were observed up to 1,000 cycles.

The electrochemical active surface area decreases only ca. 6 % after the durability tests indicating that the electrocatalysts remain active until this point. This loss in activity may be attributed to partial leaching of metals in the acidic medium.

The ORR is very slow and is usually the limiting step of the redox reactions performed in fuel cells. The mass activity values were obtained at 0.85 V potential that corresponds to the potential of a working cathode in a fuel cell. The MA_{ORR}

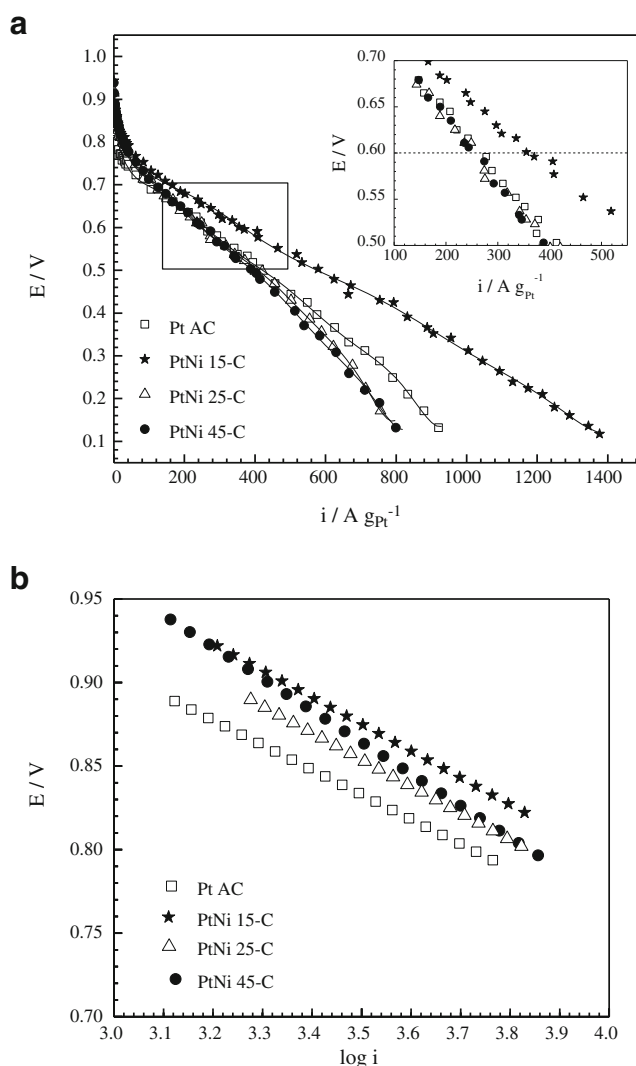


Fig. 6 Polarisation curves (a) for the Pt AC, PtNi 15-C, PtNi 25-C and PtNi 45-C. The Tafel plots at high potential values (b). Nafion® 117 membrane; air flow = 500 mL min^{-1} , H_2 flow = 100 mL min^{-1} , P_{H_2} = 1 bar, P_{air} = 2 bar. Fuel cell temperature = 80°C . Current i is expressed in Ampere per gram of platinum

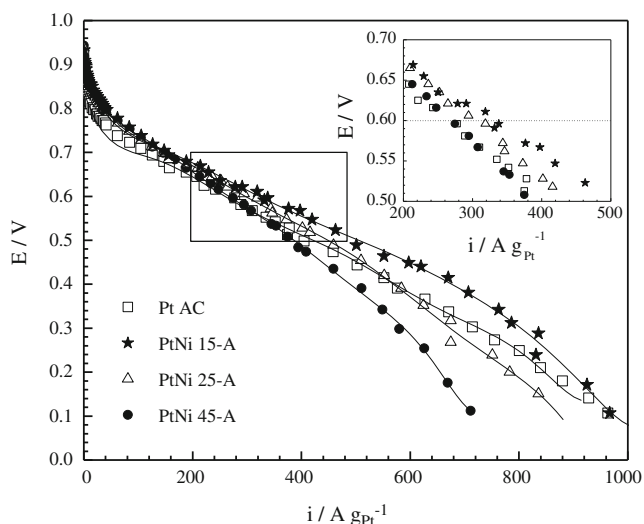


Fig. 7 Polarisation curves for the Pt AC, PtNi 15-A, PtNi 25-A and PtNi 45-A. Nafion® 117 membrane; air flow=500 mL min⁻¹, H₂ flow=100 mL min⁻¹, P_{H₂}=1 bar, P_{air}=2 bar. Fuel cell temperature=80 °C

were 447, 521, 764, and 1,027 A g_{Pt}⁻¹ for the electrocatalysts Pt/C, PtNi/C 15, PtNi/C 25 and PtNi/C 45, respectively. There was an increase in the MA_{ORR} values when nickel was incorporated into the platinum crystalline lattice. This improvement may also be related to the atomic fraction of Ni in the PtNi electrocatalysts because the Pt–Pt distance decreases and the electronic state of Pt changes when the appropriate amount of Ni is incorporated [13].

Many electrocatalysts are studied only in half-cells; however to accurately evaluate the catalytic system, the electrocatalysts must be assessed in a PEMFC [15, 19, 31, 35]. The MEA's effect was analysed by the polarisation curves (E versus i). Different MEAs were tested to evaluate the PtNi/C electrocatalysts as the anode and/or cathode as illustrated in Table 2.

Analyses of the experimental polarisation curves were performed using the semi-empirical Eq. 2 [36]:

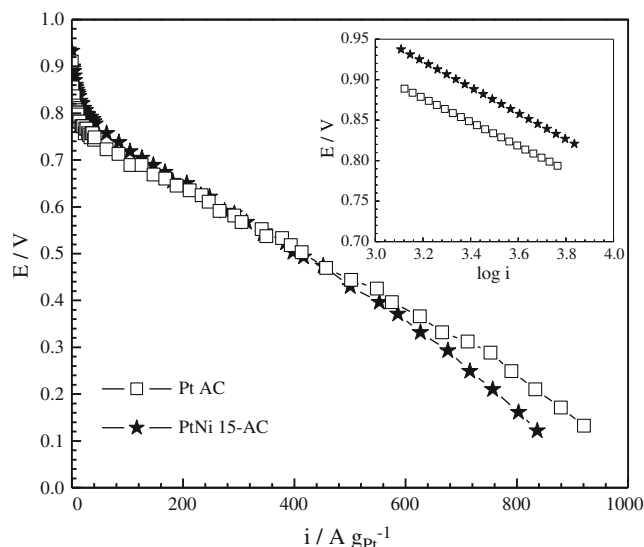


Fig. 8 Polarisation curves for the Pt AC and PtNi 15-AC. Nafion® 117 membrane; air flow=500 mL min⁻¹, H₂ flow=100 mL min⁻¹, P_{H₂}=1 bar, P_{air}=2 bar. Fuel cell temperature=80 °C. Inset: The Tafel plots at high potential values. Current i is expressed in Ampere per gram of platinum

$$E = E^0 - b \log i - Ri \quad (2)$$

where, $E^0 = E_r + b \log i_0$. E_r is the reversible potential of the fuel cell (1.229 V), b is the Tafel slope, i_0 is the exchange current for ORR in the electrocatalysts and R is the system's ohmic resistance represented by linear polarisation components. The R includes the charge transfer resistance of the hydrogen oxidation reaction, the ionic resistance of the electrolyte inside the catalyst layer and membrane, the electronic resistance and the linear diffusion terms due to diffusion limitations inside the gas diffusion layer and/or in a thin electrolyte/water film covering the electrocatalyst particles [36]. Figure 6 shows the MEAs' polarisation curves for the PtNi/C electrocatalysts in the cathode and the Pt/C electrocatalyst in the anode as well as the Tafel plots at high potentials.

Typical polarisation curves for a PEMFC with Nafion® are displayed in Fig. 6a [28]. The PtNi 15-C MEA shows higher

Table 3 Kinetic parameters (E^0 , b , R) and $i_{0.85}$, $i_{0.6}$, P_{\max} of different MEAs

MEA	E^0 V (±0.004)	b mV dec ⁻¹ (±2)	$i_{0.85}$ A g _{Pt} ⁻¹ (±0.2)	$i_{0.6}$ A g _{Pt} ⁻¹ (±2)	R Ω cm ² (±0.02)	P_{\max} W g _{Pt} ⁻¹ (±4)
Pt AC	0.862	64	3.0	260	1.37	236
PtNi 15-C	0.894	70	13.8	368	0.94	336
PtNi 25-C	0.886	70	7.0	250	1.38	218
PtNi 45-C	0.906	67	8.8	254	1.48	212
PtNi 15-A	0.907	–	–	328	1.15	276
PtNi 25-A	0.901	–	–	298	1.35	232
PtNi 45-A	0.906	–	–	268	1.65	198
PtNi 15-AC	0.893	69	12.6	262	1.44	218

values for the limiting current and a better performance than the MEAs samples containing PtNi/C or Pt/C in the cathode. In the activation-controlled region (0.75–0.95 V; Fig. 6b), the presence of Ni in the crystalline lattice directs the platinum's catalytic activity toward the oxygen reduction reaction and produces higher mass activity values. The PtNi/C electrocatalysts may promote lower adsorption strengths for the oxygenated intermediate species on the Pt surface and lower Pt–O coverage due to the faster Pt–O reduction. In addition, Pt–OH_{ad} formation is inhibited on Pt sites by the Ni oxides [19, 37]. The electrode's kinetic parameters were obtained from the experimental results reported in Figs. 6 and 7 and are presented in Table 3.

The increase in the E^0 values for nickel-containing electrocatalysts is caused by the improved reaction kinetics. The Tafel slope (b) values are near 70 mV dec⁻¹, which is the expected value for the ORR on Pt alloy electrocatalysts as previously reported [38]. The increased catalytic activity toward the ORR may also be observed by the mass activity at 0.85 V ($i_{0.85}$ V). As expected, Ni incorporated in the platinum crystalline lattice seems to favour the ORR but not in the same way as was observed in the half-cell. Interestingly, the best result found in the PEMFC at 0.85 V was using the PtNi 15-C MEA and not the PtNi 25-C or PtNi 45-C MEAs because to maintain the equivalent amounts of platinum in the PtNi/C 25 and PtNi/C 45 required a larger amount of electrocatalyst. These thicker MEAs increase the resistance of the electrode. This behaviour may be confirmed by the R values that increase with increasing Ni proportion and therefore with the increasing amount of electrocatalyst in the MEAs. Consequently, these features imply that the performance of the electrocatalyst in the PEMFC depends on the Ni proportion and on the MEA preparation method. Furthermore, the mass activity values at 0.6 V ($i_{0.6}$ V), which represents the effect of the ion flow through the electrolyte and the electron flow in the electrode were higher to the PtNi 15-C MEA as well as observed at 0.85 V. The PtNi 15-C MEA provided better results because it exhibits higher mass activity, minor ohmic resistance and, therefore, higher maximum power values relative to the other PtNi/C electrocatalysts and the Pt/C electrocatalyst.

Figure 7 shows polarisation curves for the MEAs with the PtNi/C electrocatalysts in the anode and the Pt/C electrocatalyst in the cathode. The PtNi 15-A MEA also shows higher values for the limiting current and a better performance than the MEA samples containing PtNi/C or Pt/C in the anode. The mass activity at 0.6 V are 328, 298 and 268 A g_{Pt}⁻¹ for the PtNi 15-A, PtNi 25-A and PtNi 45-A, respectively. With respect to the electrocatalysts based on PtNi/C, the Ni modifies the electronic structure of Pt improving the hydrogen oxidation reaction [39]. However, to optimise the use of Ni-based electrocatalysts, the influence of the proportion and amount of electrocatalyst in the anode must be considered. Similar to what

was observed at the cathode when increasing the amount of electrocatalyst at the anode, the electrode resistance increases and therefore reduces the maximum power of the PEMFC.

Figure 8 shows the PEMFC performance of the PtNi 15-AC MEA that contains the PtNi/C 15 electrocatalyst in both electrodes. The PEMFC of the PtNi 15-AC MEA produced lower values of the limiting current. The PtNi 15-AC MEA might maintain the $i_{0.85}$ V (12.6 A g_{Pt}⁻¹), E^0 (0.893 V) and b (69 mV dec⁻¹) values, similar to PtNi 15-C MEA, indicating that using the PtNi/C 15 in the anode did not affect the ORR. However, the PEMFC of the PtNi 15-AC MEA produced lower $i_{0.6}$ V value and maximum power than of the PtNi 15-A or PtNi 15-C MEAs. Therefore, the electrode resistance begins to influence the system because the R value was increased.

Conclusion

PtNi/C electrocatalysts were prepared by the borohydride method on a functionalised carbon support and proven effective in the cathodes or anodes of PEMFCs. Homogeneous distribution of the PtNi on the carbon support and different Ni proportion were obtained. The PEMFC performance was evaluated using PtNi/C 15 in the anode or cathode producing higher mass activity values than were observed with the Pt/C electrocatalyst. The maximum power also increased in the systems that contained the PtNi/C 15 electrocatalyst in the cathode relative to the Pt/C electrocatalyst. The electrocatalytic performance in the fuel cell depends on Ni proportions in the electrocatalysts and on the MEA preparation method. The PEMFC performance was enhanced when PtNi/C electrocatalysts were used; this effect is important by itself and has a secondary benefit: the reduction of costs because the noble metal (Pt) was partially replaced with a less expensive one (Ni).

Acknowledgments The CNPq, FAPERGS/PRONEX/CNPq and CEEE organisations are gratefully acknowledged for their financial support.

References

- Shen J, Hu Y, Li C, Qin C, Ye M (2008) Pt–Co supported on single-walled carbon nanotubes as an anode catalyst for direct methanol fuel cells. *Electrochim Acta* 53:7276–7280
- Mayrhofer KJJ, Strmcnik D, Blizanac BB, Stamenkovic V, Arenz M, Markov NM (2008) Measurement of oxygen reduction activities via the rotating disc electrode method: From Pt model surfaces to carbon-supported high surface area catalysts. *Electrochim Acta* 53:3181–3188
- Pozio A, Giorgi L, Antolini E, Passalacqua E (2000) Electrooxidation of H₂ on Pt/C Pt–Ru/C and Pt–Mo/C anodes for polymer electrolyte fuel cell. *Electrochim Acta* 46:555–561

- Santiago EI, Camara GA, Ticianelli EA (2003) CO-tolerance on PtMo/C electrocatalysts prepared by the formic acid method. *Electrochim Acta* 48:3527–3534
- Zhang Z, Xin L, Sun K, Li W (2011) Carbon supported Pd-Sn and Pd-Ru-Sn nanocatalysts for ethanol electro-oxidation in alkaline medium. *Int J Hydrogen Energy* 36:4664–4672
- Antolini E (2003) Formation of carbon-supported PtM alloys for low temperature fuel cells: a review. *Mat Chem Phys* 78:563–573
- Siracusanò S, Stassi A, Baglio V, Aricò AS, Capitanio F, Tavares AC (2009) Investigation of carbon-supported Pt and PtCo catalysts for oxygen reduction in direct methanol fuel cells. *Electrochim Acta* 54:4844–4850
- Jung DH, Lee CH, Kim CS, Shin DR (1998) Performance of a direct methanol polymer electrolyte fuel cell. *J Power Sources* 17:169–173
- Aricò AS, Stassi A, Modica E, Omelas R, Gatto I, Passalacqua E, Antonucci V (2008) Performance and degradation of high temperature polymer electrolyte fuel cell catalysts. *J Power Sources* 178:525–536
- Zhou X, Zhang R, Zhou Z, Sun S (2011) Preparation of PtNi hollow nanospheres for the electrocatalytic oxidation of methanol. *J Power Sources* 196:5844–5848
- Wu H, Wang G (2009) Pt_xNi alloy nanoparticles as cathode catalyst for PEM fuel cells with enhanced catalytic activity. *J Alloys Compd* 488:195–198
- Zhao Y, Yifeng E, Fan L, Qiu Y, Yang S (2007) A new route for the electrodeposition of platinum–nickel alloy nanoparticles on multi-walled carbon nanotubes. *Electrochim Acta* 52:5873–5878
- Min M, Cho J, Cho K, Kim H (2000) Particle size and alloying effects of Pt-based alloy catalysts for fuel cell applications. *Electrochim Acta* 45:4211–4217
- Antolini E, Salgado JRC, Gonzalez ER (2006) Oxygen reduction on a Pt₇₀Ni₃₀/C electrocatalyst prepared by the borohydride method in H₂SO₄/CH₃OH solutions. *J Power Sources* 155:161–166
- Yang H, Vogel W, Lamy C, Alonso-Vante N (2004) Structure and electrocatalytic activity of carbon-supported Pt-Ni alloy nanoparticles toward the oxygen reduction reaction. *J Phys Chem B* 108:11024–11034
- Ayoub JMS, Gerales AN, Tusi MM, Spinacé EV, Neto AO (2011) Preparation of PtSnSb/C by an alcohol reduction process for direct ethanol fuel cell (DEFC). *Ionics* 17:559–564
- Tang Y, Zhang L, Wang Y, Zhou Y, Gao Y, Liu C, Xing W, Lu T (2006) Preparation of a carbon supported Pt catalyst using an improved organic sol method and its electrocatalytic activity for methanol oxidation. *J Power Sources* 162:124–128
- Piasentin RM, Spinacé EV, Tusi MM, Neto AO (2011) Preparation of PdPtSn/C-Sb₂O₅. SnO₂ electrocatalysts by borohydride reduction for ethanol electro-oxidation in alkaline medium. *Int J Electrochem Sci* 6:2255–2263
- Zignani SC, Antolini E, Gonzalez ER (2009) Stability of Pt–Ni/C (1:1) and Pt/C electrocatalysts as cathode materials for polymer electrolyte fuel cells: effect of ageing tests. *J Power Sources* 191:344–352
- Wang G, Gao Y, Wang Z, Du C, Wang J, Yin G (2010) Investigation of PtNi/C anode electrocatalysts for direct borohydride fuel cell. *J Power Sources* 195:185–189
- Carmo M, dos Santos AR, Poco JGR, Linardi M (2007) Physical and electrochemical evaluation of commercial carbon black as electrocatalysts supports for DMFC applications. *J Power Sources* 173:860–866
- Carmo M, Linardi M, Poco JGR (2009) Characterization of nitric acid functionalized carbon black and its evaluation as electrocatalyst support for direct methanol fuel cell applications. *Appl Catal Gen* 355:132–138
- Chen M, Wang Z, Ding Y, Yin G (2008) Investigation of the Pt–Ni–Pb/C ternary alloy catalysts for methanol electrooxidation. *Electrochem Commun* 10:443–446
- Brandalise M, Tusi MM, Piasentin RM, Linardi M, Spinacé EV, Neto AO (2010) PtRu/C and PtRuBi/C electrocatalysts prepared in two different ways by borohydride reduction for ethanol electro-oxidation. *Int J Electrochem Sci* 5:39–45
- Wang Z, Zuo P, Yin G (2009) Investigation of compositions and performance of PtRuMo/C ternary catalysts for methanol electrooxidation. *Fuel Cells* 9:106–113
- de Souza RFB, Neto ET, Calegari ML, Santos EA, Martinho HS, dos Santos MC (2011) Ethanol electro-oxidation on Pt/C electrocatalysts: an “in situ” raman spectroelectrochemical study. *Electrocatal* 2:28–34
- Correa PS, da Silva EL, da Silva RF, Radtke C, Moreno B, Chinarro E, Malfatti CF (2012) Effect of decreasing platinum amount in Pt-Sn-Ni alloys supported on carbon as electrocatalysts for ethanol electrooxidation. *Int J Hydrogen Energy* 37:9314–9323
- Nagarajan M, Kalaigan GP, Paruthimal GA (2013) Novel synthesis and characterization of nanocomposite Pt-WO₃-TiO₂/C electrocatalyst for PEMFC. *Ionics* 19:127–135
- Brandalise M, Verjullo-Silva RWR, Tusi MM, Correa OV, Farias LA, Linardi M, Spinacé EV, Neto AO (2009) electro-oxidation of ethanol using PtRuBi/C electrocatalyst prepared by borohydride reduction. *Ionics* 15:743–747
- Spinacé EV, Linardi M, Neto AO (2005) Co-catalytic effect of nickel in the electro-oxidation of ethanol on binary Pt–Sn electrocatalysts. *Electrochem Commun* 7:365–369
- Fang B, Luo J, Njoki PN, Loukrakpam R, Wanjala B, Hong J, Yin J, Hu X, Last J, Zhon C (2010) Nano-engineered PtVFe catalysts in proton exchange membrane fuel cells: electrocatalytic performance. *Electrochim Acta* 55:8230–8236
- Angelucci CA, Silva MD, Nart FC (2007) Preparation of platinum–ruthenium alloys supported on carbon by a sonochemical method. *Electrochim Acta* 52:7293–7299
- Deivaraj TC, Lee JY (2005) Preparation of carbon-supported PtRu nanoparticles for direct methanol fuel cell applications—a comparative study. *J Power Sources* 142:43–49
- Antolini E, Salgado JRC, Gonzalez ER (2005) Carbon supported Pt75M25 (M=Co, Ni) alloys as anode and cathode electrocatalysts for direct methanol fuel cells. *J Electroanal Chem* 580:145–157
- Travitsky N, Ripenbein T, Golodnitsky D, Rosenberg Y, Burshtein L, Peled E (2006) Pt-, PtNi- and PtCo-supported catalysts for oxygen reduction in PEM fuel cells. *J Power Sources* 161:782–789
- Antolini E, Passos RR, Ticianelli EA (2002) Electrocatalysis of oxygen reduction on a carbon supported platinum-vanadium alloy in polymer electrolyte fuel cell. *Electrochim Acta* 48:263–270
- Santos LGRA, Oliveira CHF, Moraes IR, Ticianelli EA (2006) Oxygen reduction reaction in acid medium on Pt–Ni/C prepared by a microemulsion method. *J Electroanal Chem* 596:141–148
- Negro E, Noto VD (2008) Polymer electrolyte fuel cells based on bimetallic carbon nitride electrocatalysts. *J Power Sources* 178:634–641
- Cho Y, Cho Y, Lim J, Park H, Jung N, Ahna M, Choe H, Sung Y (2012) Performance of membrane electrode assemblies using PdPt alloy as anode catalysts in polymer electrolyte membrane fuel cell. *Int J Hydrogen Energy* 37:5884–5890